AD-A054 318 WAYNE STATE UNIV DETROIT MI DEPT OF ELECTRICAL ENGIN--ETC F/G 20/8
TRANSFERRED ELECTRON EFFECTS IN N-GAAS AND N-INP UNDER HYDROSTA--ETC(U).
APR 78 W CZUBATYJ, M S SHUR, M P SHAW N00014-75-C-0392

UNCLASSIFIED NL

| OF |
AD
A054318

END
DATE FILMED
6 -78
DDC

Transferred Electron Effects In N-GaAs And N-InP Under Hydrostatic Pressure,

Wolodymyr Czubatyj, M.S./Shur M.P. Shaw
Department of Electrical Engineering
Wayne State University
Detroit, Michigan 48202

4 APR 78

This report summarizes the research carried out during the past three years under ONR contract N00014-75-C-0392. The details of the experimental work can be found in the Wayne State University Ph.D. Dissertation of Wolodymyr Czubatyj, 1977, Department of Electrical and Computer Engineering. The important conclusions, both experimental and theoretical, are contained in the attached reprints, which comprise the major portion of this report.

In brief, we experimentally investigated transferred electron effects in bulk n-GaAs and n-InP under hydrostatic pressures, and compared the results with the results of our numerical Monte Carlo calculations. Our experimental results differed substantially from those of other investigators, and our numerical results showed that the discrepancies were due to the presence of substantial ionized impurity scattering in our samples. In general, we not only verified that fundamental band structure effects are masked by contact phenomena, but also that they are seriously affected by ionized impurity scattering.

To obtain useful results for fundamental band structure parameters using transferred electron effects, the investigator must begin with high purity, high mobility material, relatively free from ionized impurities. This can usually be achieved by epitaxial growth. The epitaxial samples should be grown on a semi-insulating substrate and shaped into 'H' or turret patterns to minimize effects → over

due to the metallic contacts. Turret shaped samples are best since in one polarity a boundary condition producing either transit time oscillations or current saturation due to a high cathode field will yield values of the saturated drift velocity. In the opposite polarity, the absence of a domain mode and a sufficiently high value of the peak velocity, along with current saturation or switching, or circuit controlled oscillations, can then provide confidence that low boundary field conditions have been achieved.

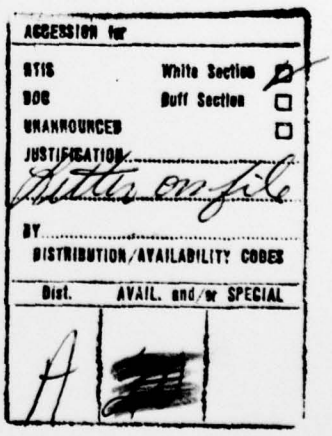

Solid-State Electronics, 1978, Vol. 21, pp. 75–78. Pergamon Press. Printed in Great Britain

TRANSFERRED ELECTRON EFFECTS IN *n*-GaAs AND *n*-InP UNDER HYDROSTATIC PRESSURE†

W. CZUBATYJ, M. S. SHUR and M. P. SHAW

Department of Electrical and Computer Engineering, Wayne State University, Detroit, MI 48202, U.S.A.

Abstract—Experimental results are presented showing the variation of the peak velocity, electric field at peak velocity and saturated velocity of the velocity-field curve for bulk *n*-GaAs under hydrostatic pressure. Similar data are presented for the field at peak velocity for bulk *n*-InP. The extraction of the data from the current-voltage characteristics is based on an exploitation of the influence of boundary conditions on the manifestation of transferred-electron induced (Gunn) current instabilities. Our results, which differ from those of other investigations, are compared with our Monte Carlo calculations of the velocity-field curves for these materials. We find that ionized impurity scattering plays an important role in the understanding of our data.

1. INTRODUCTION

Two recent experimental investigations of the high electric field transport properties of *n*-GaAs[1, 2] and *n*-InP[3] under hydrostatic pressure have helped provide further clarification of the position and variation with pressure of some conduction band extrema in these materials. Furthermore, Vinson *et al.*[1] have also made uniaxial stress measurements and obtained numerical evidence supporting the view that the lowest subsidiary minimum in the conduction band of GaAs lies at the *L* point in the Brillouin zone[4]. In the above investigation, the high quality material employed was epitaxially grown from the vapor phase onto n^+ substrates and the top contact was an alloyed metal (Sn or Ag–Sn) uniformly covering the entire active region. In our studies we have used less pure, long bulk (horizontal Bridgman and Czochralski) samples where contact effects have been minimized by geometrically shaping the sample to remove the active region from the influence of the cathode contact. Although both sets of results exhibit some of the same qualitative features, there are sufficient *substantial* quantitative differences so that it is difficult to obtain an unambiguous interpretation of the data. These differences will be emphasized in the following two sections where our experimental results are presented. In the last section we discuss the results of our numerical calculations, which demonstrate that ionized impurity scattering plays an important role in controlling the character of our experimental results.

2. EXPERIMENTAL RESULTS FOR *n*-GaAs

The experimental studies involve applied voltages sufficiently high to induce the Gunn instability[5]. Vinson *et al.*[1] and Pickering *et al.*[2] have both observed that the threshold voltage, V_t, for the Gunn instability increases with applied hydrostatic pressure, P, in the range from 0 up to about 15 kbar. At higher values of P, V_t first decreases then increases with P until the instability disappears near 30 kbar. The observation of a range where V_t decreases with P is consistent with the original observations of Hutson *et al.*[6]. It was demonstrated by Pickering *et al.* that the failure to observe an initial increase in V_t with P by Hutson *et al.* was due to the nonlinear type of alloyed metal-semiconductor used. Recently, we pointed out[7] that even with the linear metal-semiconductor contacts employed by Vinson *et al.* and Pickering *et al.*, major features of the velocity-field, $v(E)$, characteristics may still be masked. We found that once the controlling influence of the contacts were eliminated, the *field at peak velocity*, E_p, (see Fig. 1) was found to increase *substantially* with P up to near 10 kbar. Furthermore, the peak velocity, v_p, and saturated velocity, v_s, also increased as well.

Our experimental and numerical results, as well as those of Vinson *et al.*, are summarized in Fig. 1. To obtain our experimental results, it was necessary to shape (sculpture) the sample as shown in the inset. The reason for this is that unless the cathode boundary contact fields are reduced below E_p[5, 7], a transit-time instability will occur at currents *below* the current density j_p associated with v_p. Samples that were not sculptured produced either current saturation or transit-time effects.

Our specimens were cut from previously metallized and alloyed wafers of [111] oriented bulk material having carrier concentrations in the range $1.7\text{–}2.3 \times 10^{15}\ \text{cm}^{-3}$ and mobilities in the range 3000–5500 cm^2/V-sec. All our samples exhibited an exponential increase in resistance with P, beginning above about 1 kbar, which we attributed to carrier freeze-out to impurity levels as the band gap increased. This phenomenon makes the data analysis more difficult and the results somewhat less precise, but, as we shall show, the results were consistent with our assumptions.

The contacts were formed by first evaporating onto the samples a thin coat of Sn(~500Å thick), then electrolessly depositing Ni(~1000Å thick), and finally evaporating another layer of Sn(~12,000Å thick). The samples were then alloyed for typically three minutes at 500°C. They were diced into parallelopipeds approximately $0.10 \times 0.10 \times 0.04$ cm on edge. Finally, each parallelopiped was sculptured into the form shown in the inset of Fig. 1 by using a wire string saw coated with abrasive grit. When the smaller contact was the cathode the current saturated at a value $j_s = nev_s$[5], where ne is the charge density. When

†Research supported by the Office of Naval Research under Contract No. N-0014-75-C-0399.

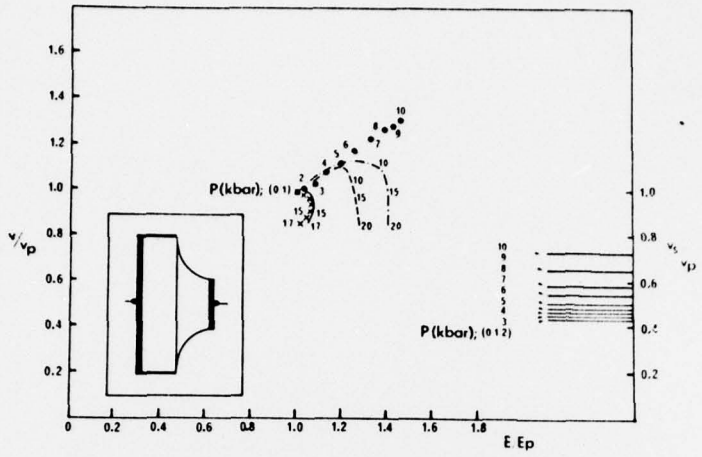

Fig. 1. Normalized peak velocity (dots) and saturated velocity (straight lines) vs normalized electric field at peak velocity as a function of P for GaAs. The data were extracted from $I(V)$ curves for three samples taken with 100 nsec voltage pulses at a prf of 50 hz. For a typical sample $v_p = 1.97 \times 10^7$ cm/sec and $E_p = 4800$ V/cm. The crosses beginning at the $P = 0$ point represent an average of the data appearing in Ref. 1. The curved solid line represents an average of the numerical results we obtained and those of Ref. 1; $N_t = 0$. The dashed line shows our numerical results for $N_t = 10^{17}$ cm^{-3}. The dot-dashed line shows our numerical results for $N_t = 10^{18}$ cm^{-3}. The inset displays the shape of a typical sample, drawn to scale. The pre-sculptured dimensions are given in the text. Sculpturing typically reduced the cross-sectional area by about a factor of 7.

the larger contact was the cathode (here the active region is effectively removed from the influence of the cathode contact), the $I(V)$ characteristics were linear up to v_p.

After the $I(V)$ measurements were made, the samples were mounted by their leads on a transistor header, immersed in epoxy, capped and centrifuged to remove any bubbles present in the epoxy. They were then placed in a core drilled from the center of a cut pyrophylite regular tetrahedron, 2.54 cm on edge. The core voids were filled with a Duco-rouge mixture and the pyramid rouged and placed into a tetrahedral press capable of achieving pressures up to 40 kbar. The system was calibrated and checked for hydrostatic behavior by replacing the GaAs samples with Bi, Ce, Hg, or Yb, and recording the P-induced phase transitions in these materials.

The $I(V)$ curves for both polarities were measured at 1 kbar intervals up to 12 kbar and the data analysis proceeded as follows. First, at atmospheric P, the low-voltage resistance, R, of the sample, V_t, I_p, and I_s were measured, where I_p and I_s are the peak and saturated currents, respectively. The ratio I_p/I_s yielded v_p/v_s directly. v_p was obtained by using the value $v_s = 0.86 \times 10^7$ cm/sec. This fixes E_p [5, 7] and hence the mobility $\mu (= v_p/E_p)$. The carrier density, n, was then determined from the resistivity, ρ, measured prior to sculpturing. j_p was calculated ($= nev_p$) and the effective cross-sectional area A of the active region was then determined ($= I_p/j_p$). The pseudo-sample-length l was taken as V_t/E_p. (Both l and A are expected to remain constant to within 1–2% up to 12 kbar.)

Next, as P was increased we determined $\rho (= RA/l)$, n (using the fact that μ will decrease by about 10% from 0 to 10 kbar, [8] which we checked experimentally for self-consistency), j_p, v_s, $v_p' (= j_p/ne)$, E_p, $E_p' (= v_p'/\mu)$ and $\mu' (= v_p'/E_p)$. The primes denote an alternate method of obtaining these parameters. Comparison of v_p with v_p', E_p with E_p' and μ with μ' provided a critical check of our technique. The agreement was never worse than 15% and typically good to within 5%. Each datum point plotted in Fig. 1 is an average of the primed and unprimed data. The sources of error are uncertainties in changes of physical dimensions with pressure (2%), P(5%), I and V (3%), and ρ (10%). It is evident that v_p, E_p, and v_s all increase substantially with P up to 10 kbar. It is evident that v_p, E_p, and v_s all increase substantially with P up to 10 kbar. In the data shown in Fig. 1 the turnover point (where [v_p, E_p] starts decreasing with P) is near 10 kbar. However, the high R of the sample at these P's make the turnover point difficult to determine accurately.

3. EXPERIMENTAL RESULTS FOR n-InP

Pitt and Vyas [3] found that V_t for the Gunn instability in InP remained constant for pressures up to near 40 kbar. After that V_t increased with P up to about 70 kbar. Our results, which are startlingly different, are shown in Fig. 2. To obtain these results, the InP samples were prepared almost exactly as the GaAs samples. However, the "turret" type samples shown in the inset of Fig. 1 were extremely hard to fabricate since InP is very fragile and cracks under the slightest stress along the (100) plane. Even when a sample was successfully fabricated, it was found that it could not be cycled electrically because the high fields often present at the small contact caused irreversible damage. Therefore, a different design was tried in order to reduce the fields at *both* electrodes. Two deep cuts were made into the sample with one surface contract removed (see inset of Fig. 2). (Such a large contact area-double cut sample proved to be stable under hydrostatic pressure. Voltage probing of Teledel-

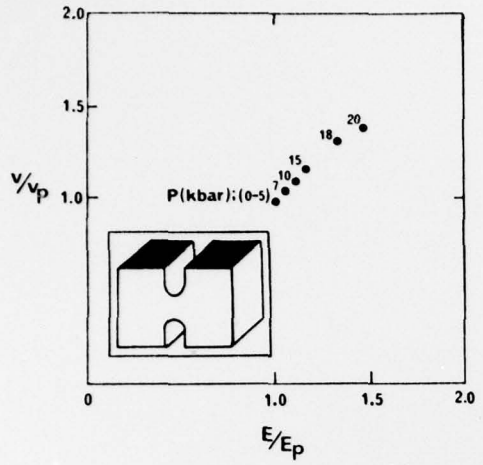

Fig. 2. Normalized peak velocity vs normalized electric field at peak velocity as a function of P for InP. The inset displays the shape of a typical sample, drawn to scale.

tos resistance paper cut to model the cross-sectional shape of an actual sample showed that approximately half of the applied voltage was dropped in the central region and the remainder in the bulk.) When the applied bias was increased, the voltage drop in the central region would correspondingly increase. Due to the large area of the contact region, only a small voltage was dropped there. Only at very large voltages, approximately two or three times larger than the peak voltages used, does the cathode drop become significant (25 to 33% of the sample voltage). Upon reaching the peak current for the sample, the central region began to avalanche rapidly, producing in a short time a sample of lower resistance, and yielding an increased current and smaller voltage drop across the central region. If the fields at the contacts were relatively small at the time of this switching effect, the switching occurred along the load line to a stable, *higher* current point. If, however, the contact fields were too large when the switch occurred and the redistributed voltage caused breakdown in these regions, irreversible damage would occur. Several samples were destroyed in this manner.

The data taken for the sculptured InP samples (Fig. 2) were similar to those of GaAs, except that the "current saturation polarity" was absent because the samples were symmetric. Even in unsculptured samples that could have shown saturation for lower carrier concentrations, impact ionization within the high cathode field region always caused the current to rise continuously with increasing voltage, making determination of a saturated current impossible. The curves also had a "soft" knee, making determination of the knee point an unreliable process. In general, unsculptured bulk InP samples ($n \geq 2 \times 10^{15}\,\mathrm{cm}^{-3}$) develop sufficiently high cathode fields so that the current observed on a sampling oscilloscope will usually increase as the voltage increases, even when a domain instability is generated.

Our samples had carrier concentrations typically in the range $2\text{–}4 \times 10^{15}\,\mathrm{cm}^{-3}$ and mobilities between 3500 and $4500\,\mathrm{cm}^2/\mathrm{V\text{-}sec}$. The resistivity varied from about 0.4 to 0.6 Ω-cm. In order to avoid cumulative breakdown effects in these samples, we applied *single-shot* voltage pulses. As the applied bias brought the current to near the peak value, the $I(V)$ curves developed a small sublinearity, which is expected for InP since its $v(E)$ curve is sublinear prior to threshold (GaAs is linear). At the peak current, a switch to higher current occurs along the load line. We attribute this effect to impact ionization within the anode high field region[5].

The peak current density $J_p = I_p/A$, where A is known to within 10% and I_p to within 3%, yielded a value for n, assuming a given value for v_p. This also yielded a corresponding μ from the $v(E)$ curve for InP obtained by Fawcett and Herbert[9]. The resistivity was then measured, and the process iterated until good agreement between v_p, μ n and ρ was obtained.

As for GaAs, ρ as a function of P was obtained. Next, J_p/ne yielded v_p as a function of P. E_p as a function of P was obtained by dividing V_t by a constant determined by the width of the cut and a geometric sculpturing factor. The data presented in Fig. 2 represents an average of three samples.

4. NUMERICAL CALCULATIONS AND DISCUSSION

In order to explain the above data, we performed Monte Carlo calculations of the $v(E)$ characteristics. In this paper we will emphasize our results for GaAs. We used essentially the same parameters used in Ref. 1: Effective mass-$m_\Gamma^* = 0.68m_0$, $m_x^* = 0.35m_0$, $m_L^* = 0.35m_0$; Energy separation-$\Delta E_{\Gamma-x} = 0.40\mathrm{eV}$, $\Delta E_{\Gamma-L} = 0.38\,\mathrm{eV}$; Pressure dependence of the energy separations, $(\mathrm{d}E_{\Gamma-x}/\mathrm{d}P) = -11 \times 10^{-6}\,\mathrm{eV\,bar}^{-1}$, $(\mathrm{d}E_{\Gamma-L}/\mathrm{d}P) = -5 \times 10^{-6}\,\mathrm{eV\,bar}^{-1}$; Deformation potential $-7\,\mathrm{eV}$; Coupling constants—the unscreened values of Ref. 9; Pressure dependence of effective mass, $(\mathrm{d}m_\Gamma^*/\mathrm{d}P)$ from $k \cdot p$ theory with $(\mathrm{d}E_\kappa/\mathrm{d}P) = 10 \times 10^{-6}\,\mathrm{eV\,bar}^{-1}$ and m_x^*, m_Γ^* constant. (E_κ is the energy gap and Γ, $\times$, L are major symmetry points in the Brilloiun zone.) Using these parameters with parabolic bands, and considering acoustic, optical, intervalley and intravalley scattering, we were able to reproduce the numerical results of Ref. 1 reasonably well (see Fig. 1). *Only when we included ionized impurity scattering* at a density greater than about $N_I = 10^{17}\,\mathrm{cm}^{-3}$ were we able to obtain results that were similar to ours; an initial increase in v_p and a relatively large initial increase in E_p with increasing P (see Fig. 1). (The use of the band parameters suggested by Aspnes[4] made the agreement between experiment and numerical calculation more disparate.) Note that v/v_p remains above unity over a larger range of P for larger values of N_I. E/E_p is also greater at a given P for larger values of N_I.

We suggest the following model in order to explain the role that ionized impurity scattering plays in controlling the variation of the (v_p, E_p) point with P. First, we know that E_p increases as μ decreases. Furthermore, since μ decreases with increasing P, $(\mathrm{d}E_p/\mathrm{d}P)$ will be greater for smaller μ in the range where E_p increases with P. Since μ decreases as N_I increases, we expect that both E_p and

its variation with P to increase with increasing N_I.

Next, in order to explain why v_p increases with increasing P, we assume that the average drift velocity is given by $v = (n_L v_L + n_u v_u)/(n_L + n_u)$, where v_L, n_L and v_u, n_u are the drift velocities and electron concentrations in the lower and upper valleys, respectively. Since negative differential mobility is a "tail of the distribution effect", then we expect that near threshold $n_u \ll n_L$; also $v_u \ll v_L$. Hence, near threshold, $v \simeq v_L n_L/(n_L + n_u)$.

We know that impurity scattering decreases v_L. Furthermore, the value of n_u near threshold will be rather insensitive to impurity scattering, which is most important at low electron energies[10]. Thus, at atmospheric P we expect and observe a lower value of the peak velocity when impurity scattering is present than in its absence[5, 11]. At low P our calculations show that P increases E_p, with or without ionized impurity scattering. At high fields (near threshold), the difference between v_L in the presence of, and without ionized impurity scattering becomes smaller (in the limit of very high fields both values should be equal). This will result in an initial increase of v_p with P in the presence of impurity scattering. The maximum value of v_p reached under applied P will of course be below that corresponding to the situation without impurity scattering.

In summary, we have verified one, and uncovered another phenomenon which tends to mask fundamental band structure effects in negative differential mobility (NDM) semiconductors. The new effect is that of ionized impurity scattering. Ionized impurity scattering affects the peak velocity and field at peak velocity, making accurate determinations of band structure variations with pressure difficult to achieve. The second effect is that of the influence of the contacts on the form and stability of the current-voltage characteristics of NDM semiconductors subjected to hydrostatic pressure[2, 3, 7].

To improve on the results obtained for GaAs and InP, we should start with much purer, higher mobility material, relatively free of ionized impurities. This can be achieved by epitaxial growth. The expitaxial samples should be grown on a semi-insulating substrate and shaped into "H" or turret patterns to minimize (or eliminate) the metallic contact effects. The turret shaped samples (inset, Fig. 1) are most useful since in one polarity a boundary condition producing either transit-time oscillations or current saturation due to a high cathode field will yield values of v_s. In the opposite polarity, the absence of a domain mode and a sufficiently high value of v_p, along with current saturation or switching, or circuit controlled oscillations, can then provide confidence that low boundary field conditions have actually been achieved[5].

Acknowledgements—M. P. Shaw is grateful to A. Adams for very helpful conversations and correspondence. We also thank R. Jeffery and D. Gustafson for experimental assistance and guidance, and D. Ferry for a useful suggestion.

REFERENCES

1. P. J. Vinson, C. Pickering, A. R. Adams, W. Fawcett and G. D. Pitt, *Proc. 13th Int. Conf. Phys. of Semiconductors* (Edited by F. G. Fumi), p. 1243. Tipografia Marves, Rome (1976).
2. C. Pickering, A. R. Adams, G. D. Pitt and M. K. R. Vyas, *J. Phys. C.* **8**, 129 (1975).
3. G. D. Pitt and M. K. R. Vyas, *J. Phys C* **8**, 138 (1975).
4. D. E. Aspnes, *Phys. Rev.* **B14**, 5331 (1976).
5. See, e.g., P. R. Solomon, M. P. Shaw, H. L. Grubin and R. Kaul, *IEEE Trans. Electron. Dev.* **ED-22**, 127 (1975).
6. A. R. Hutson, A. Jayaraman, A. G. Chynoweth, A. S. Coriell and W. C. Feldman, *Phys. Rev. Lett.* **14**, 639 (1965).
7. W. Czubatyj and M. P. Shaw, *Appl. Phys. Lett.* **30**, 205 (1977).
8. G. D. Pitt and J. Lees, Proc. of Les Propriétiés Physiques des Solids Sous Pression, p. 225. Centre National de La Recherche Scientifique, Paris, (1970).
9. W. Fawcett and D. C. Herbert, *J. Phys.* **C7**, 1641 (1974).
10. L. Zanfi, A. Losi, C. Jacoboni and C. Canali, *IEEE Trans. Electron. Dev.* **ED-24**, 281 (1977).
11. J. G. Ruch and W. Fawcett, *J. Appl. Phys.* **41**, 3843 (1970).

Transferred-electron effects in *n*-GaAs under hydrostatic pressure*

W. Czubatyj and M. P. Shaw

Department of Electrical and Computer Engineering, Wayne State University, Detroit, Michigan 48202
(Received 15 October 1976)

Experimental results show that the peak velocity, peak electric field, and saturated velocity of the velocity–electric-field curve for *n*-GaAs all increase substantially with increasing hydrostatic pressure up to about 10 kbar; the peak velocity and field then begin decreasing with further increase in pressure. The extraction of the data from the current-voltage characteristics is based on an exploitation of the influence of the boundary conditions on the manifestation of transferred-electron-induced (Gunn) current instabilities.

PACS numbers: 72.20.Ht, 72.80.Ey

Vinson *et al.*[1] have presented numerically supported experimental evidence, based on hydrostatic pressure and uniaxial stress measurements at applied voltages sufficiently high to induce the Gunn instability,[2] in harmony with the recent finding that the lowest subsidiary minimum in the conduction band of GaAs lies at the L rather than the X point in the Brillouin zone.[3] In this paper we present further experimental evidence relating to this view and also provide additional data which for the first time displays major features of the variation of the carrier velocity v versus electric field E characteristic at hydrostatic pressures P below 12 kbar. Vinson *et al.* and Pickering *et al.*[4] have both observed that the threshold voltage V_T for the Gunn instability increases with increasing hydrostatic P in the range from 0 up to about 15 kbar. At higher values of P, V_T first decreases then increases with P until the instability disappears near 30 kbar. The observation of a range where V_T decreases with P is consistent with the original observations of Hutson *et al.*[5] It was demonstrated by Pickering *et al.* that the failure to observe an initial increase in V_T with P by Hutson *et al.* was due to the nonlinear type of alloyed metal-semiconductor contacts used. A major point of our paper is that even with the linear alloyed metal-semiconductor contacts employed by Vinson *et al.* and Pickering *et al.* the major features of the $v(E)$ characteristics are still masked. Our results show that once the influence of the contacts[6] is (i) *eliminated* and (ii) *controlled*, not only is the threshold *field* E_p observed to increase *substantially* with P up to near 10 kbar but, surprisingly, the threshold velocity v_p and saturated velocity v_s (see Fig. 1) also increase as well.

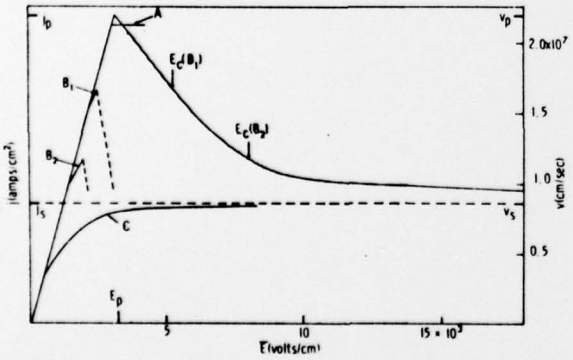

FIG. 1. The $v(E)$ curve and computer generated j-vs-$\bar{E}$ (average field) curves (A, B_1, B_2, C) for various values of E_c. E_c(A) = 0, $E_c(B_1)$ = 6 kV/cm, $E_c(B_2)$ = 8.5 kV/cm, and E_c(C) = 24 kV/cm. Curve A results for low E_c, curve C for high E_c, and curves B_1 and B_2 for intermediate E_c (in the NDM region; shaded. When E_c is in the shaded region, the cathode-to-anode transit-time instability occurs). The reason curve A does not extend up to v_p is that small statistical doping fluctuations were included in the calculations. The left- and right-hand ordinates are related by $j = n_0 e v(E)$, where n_0 is the doping density and e the electronic charge. This figure is taken from Refs. 2 and 6, where it was demonstrated that the calculations, based on a fixed E_c model, provide excellent agreement with experimental results on long samples of *n*-GaAs.

Crucial to our arguments is the fact that the classic Gunn instability, i.e., the cathode-to-anode transit-time mode,[2] does not occur at a critical value of voltage *or* electric field. In fact, trying to extract useful information from a variation in V_T for this type of instability is a futile exercise. The instability occurs at a critical value of *current density* j_c,[2,6,7] which is controlled by the value of the electric field in the negative differential mobility (NDM) region at the cathode boundary E_c. As shown in Fig. 1, if E_c is too high (above the NDM region) the transit-time instability is suppressed and the current saturates at the value $j_s = n_0 e v_s$; a high-field region remains at the cathode. In order to reach a critical current equal to j_p (from which v_p can be obtained), low-field boundary conditions must be achieved. However, the cathode-to-anode transit-time instability is also almost always suppressed for low E_c; here a high-field region often evolves at the anode and the current saturates very near $j_p = n_0 e v_p$ (Fig. 1).

We have exploited the latter two boundary conditions[2,6] (*controlling* and *eliminating*, respectively, the influence of the contacts) in order to obtain v_p, E_p, and v_s as functions of P. For our purposes the most important of these boundary conditions is that of low E_c. We have only rarely found an alloyed metal-semiconductor contact (for carrier concentrations in the mid-10^{15} cm^{-3} range and below) that produced what could be characterized as a low E_c contact. We were only able to reliably achieve this boundary condition by sculpturing the sample to remove the active region from the influence of the contacts.[6] Samples that were not sculptured pro-

duced either current saturation or transit-time effects; transit-time-type samples (intermediate E_c; within the NDM region) become electrically unstable before v_p is approached and hence cannot yield information concerning the peak point (v_p, E_p). This is an important feature. Guétin and Schréder[8] showed that the height of a Schottky barrier on n-GaAs increases with increasing P, implying that E_c increases. Thus, we expect E_c to increase with P for intermediate E_c samples. A larger E_c implies a lower j_c, which means that the critical current density for such samples will decrease with increasing P while V_T can increase. Such behavior has been emphasized in Refs. 1 and 3, and plays a major role in their analyses.

Our specimens were cut from previously metallized and alloyed wafers of [111]-oriented bulk material having carrier concentrations in the range 3000−5500 $cm^2/V sec$. All our samples exhibited an exponential increase in resistance with P, beginning above about 1 kbar, which we attributed to carrier freeze-out to impurity levels as the band gap increased. This phenomenon makes the data analysis more difficult and the results somewhat less precise, but, as we shall show, the results were consistent with our assumptions.

The contacts were formed by first evaporating onto the samples a thin coat of Sn (~ 500 Å thick), then electrolessly depositing Ni (~ 1000 Å thick), and finally evaporating another layer of Sn (~ 12 000 Å thick). The samples were then alloyed for typically 180 sec at 500 °C. They were diced into parallelopipeds approximately $0.1 \times 0.1 \times 0.04$ cm on edge. Finally, each parallelopiped was sculptured into the form shown in the inset of Fig. 2 by using a wire string saw coated with abrasive grit. When the smaller contact was the cathode, the current-voltage $I(V)$ characteristics were like those of Fig. 1, curve C (high E_c). When the larger contact was the cathode (here the active region is effectively removed from the influence of the cathode contact), the $I(V)$ characteristics were those of Fig. 1, curve A (low E_c).

After the $I(V)$ measurements were made, the samples were mounted by their leads on a transistor header, immersed in epoxy, capped, and centrifuged to remove any bubbles present in the epoxy. They were then placed in a core drilled from the center of a cut pyrophylite regular tetrahedron, 2.54 cm on edge. The core voids were filled with a Duco-rouge mixture and the pyramid rouged and placed into a tetrahedral press capable of achieving pressures up to 40 kbar. The system was calibrated and checked for hydrostatic behavior by replacing the GaAs samples with Bi, Ce, Hg, or Yb, and recording the P-induced phase transitions in these materials.

The $I(V)$ curves for both polarities were measured at 1 kbar intervals up to 12 kbar and the data analysis proceeded as follows. First, at atmospheric P, the low-voltage resistance R of the sample, I_p, V_T, and I_s were measured. The ratio I_p/I_s yielded v_p/v_s directly. v_p was obtained by using the value $v_s = 0.86 \times 10^7$ cm/sec. From the Butcher-Fawcett $v(E)$ curve (Fig. 1) this fixes E_p and hence the mobility μ $(= v_p/E_p)$. The carrier density n was then determined from the resistivity ρ measured prior to sculpturing. j_p was calculated $(= nev_p)$ and the effective cross-sectional area A of the active region was then determined $(= I_p/j_p)$. The pseudo-sample-length l was taken as V_T/E_p. (Both l and A are expected to remain constant to within 1−2% up to 12 kbar.)

Next, as P was increased we determined ρ $(= RA/l)$, n (using the fact that μ will decrease by about 10% from 0 to 10 kbar,[9] which we checked experimentally for self-consistency), j_p, v_s, v_p, v'_p $(= j_p/ne)$, E_p, E'_p $(= v_p/\mu)$, and μ' $(= v'_p/E_p)$. The primes denote an alternate method of obtaining these parameters. Comparison of v_p with v'_p, E_p with E'_p, and μ with μ' provided a critical check of our technique. The agreement was never worse than 15% and typically good to within 5%. Each datum point plotted in Fig. 2 is an average of the primed and unprimed data. The sources of error are uncertainties in changes of physical dimensions with pressure (2%), P (5%), I and V (3%), and ρ (10%). It is evident that v_p, E_p, and v_s all increase substantially with P up to 10 kbar. In the data shown in Fig. 2 the turnaround point (where $[v_p, E_p]$ starts decreasing with P) is at ~ 10 kbar. However, the high R of the sample at these P's make the turnover point difficult to determine accurately.

For comparison we also studied the affect of P on samples having intermediate E_c's. V_T either remained constant or decreased slightly as P increased to 10 kbar. Again, no information about the point (v_p, E_p) can be extracted from intermediate E_c samples.

Vinson *et al.* show that Monte Carlo calculations using L as the lowest subsidiary minimum provide good agreement with the observations that hydrostatic P initially increases E_p and uniaxial stress measurements produce decidedly different behavior for surfaces containing (100) and (111) crystallographic planes. Our

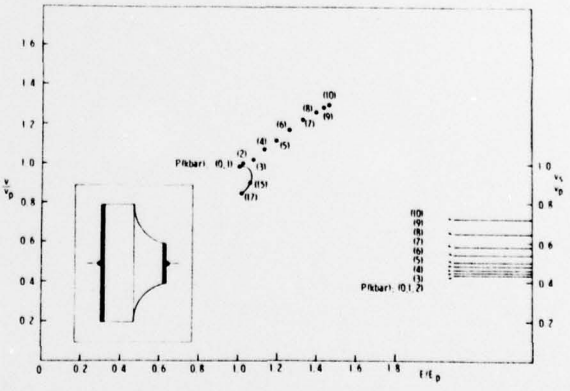

FIG. 2. Normalized peak velocity (dots) and saturated velocity (straight lines) versus normalized peak electric field as a function of P. The data were extracted from $I(V)$ curves for three samples taken with 100-nsec voltage pulses at a prf of 50 Hz[2]. For a typical sample $v_p = 1.97 \times 10^7$ cm/sec and $E_p = 4800$ V/cm. The curved line beginning at the $P = 0$ point represents an average of the data appearing in Ref. 1. The inset shows the shape of a typical sample, drawn to scale. The presculptured dimensions are given in the text. Sculpturing typically reduced the cross-sectional area by about a factor of 7.

hydrostatic P results are in fair qualitative agreement with their E_p values (which they obtain, inappropriately, from V_T) but disagree with their results for v_p, which have v_p decreasing smoothly with P (Fig. 2). Furthermore, our results show that dE_p/dP is much larger than they thought. Because of these discrepancies, the results of their uniaxial stress measurements must also be held as questionable since in those cases the samples were also not shaped to eliminate contact effects.

Without numerical calculations, it is difficult to understand our data in terms of the known band structure of GaAs. The (v_p, E_p) point is observed to increase very rapidly with P, faster than would be expected solely from an increase in effective mass in the lowest minimum (Γ). It is known that, with respect to the valence-band maximum, the Γ point increases rapidly with P ($dE/dP|_\Gamma \approx 11\times10^{-3}$ eV/kbar) and the X point decreases slowly with P ($dE/dP|_x \sim -1\times10^{-3}$ eV/kbar).[4,9,10] It is also thought that the L point increases with P, but at a rate slower than the rate of rise of Γ.[10] If this is the case, the Γ-L separation will decrease with P and hence, based on these simple arguments, (v_p, E_p) should decrease. Clearly an appreciation of the coupling constants and their P dependence is required and, in view of the recent findings of Aspnes *et al.*[3], perhaps the motion of the conduction-band extrema with P should be reexamined.

In conclusion, two points are evident. First, as previously stated, our data were taken on samples whose resistance increased exponentially starting above about 1 kbar. This behavior might lower the mobility by changing the amount of impurity scattering (which is relatively unimportant at 300°K). Because of this possibility, the changes in v_p and v_s with P might actually be smaller than indicated. However, the measured changes in E_p would be unaffected since they are taken directly off the raw data. For further verification, the experiments should be redone with sculptured bulk or shaped epitaxial samples where P-induced carrier freeze-out is but a minor effect. Second, the Monte Carlo calculations should be repeated in an attempt to fit our data. We have initiated such a program.

M. P. Shaw is grateful to A. Adams, W. Paul, and P. Vinson for useful conversations. The authors would also like to thank R. Jeffery and D. Gustafson for experimental assistance and guidance.

*Research supported by the Office of Naval Research under contract No. N-0014-75-C-0399.

[1] P.J. Vinson, C. Pickering, A.R. Adams, W. Fawcett, and G.D. Pitt, Proc. 13th Int. Conf. Phys. Semiconductors, Rome, 1976 (unpublished).
[2] See, e.g., P.R. Solomon, M.P. Shaw, H.L. Grubin, and R. Kaul, IEEE Trans. Electron Devices ED-22, (1975).
[3] D.E. Aspnes, C.G. Olson, and D.W. Lynch, Phys. Rev. Lett. 37, 766 (1976).
[4] C. Pickering, A.R. Adams, G.D. Pitt, and M.K.R. Vyas, J. Phys. C 8, 129 (1975).
[5] A.R. Hutson, A. Jayaraman, A.G. Chynoweth, A.S. Coriell, and W.C. Feldman, Phys. Rev. Lett. 14, 639 (1965).
[6] M.P. Shaw, P.R. Solomon, and H.L. Grubin, IBM J. Res. Dev. 13, 587 (1969).
[7] H.L. Grubin, M.P. Shaw, and P.R. Solomon, IEEE Trans. Electron Devices ED-20, 63 (1973).
[8] P. Guétin and G. Schréder, Phys. Rev. B 5, 3979 (1972).
[9] G.D. Pitt and J. Lees, *Proc. of Les Propriétés Physiques des Solides Sous Pression* (Centre National de la Recherche Scientifique, Paris, 1970), p. 225.
[10] D.L. Camphausen, G.A.N. Connell, and W. Paul, Phys. Rev. Lett. 26, 184 (1976).